Physical Basis for Long-Lived Electronic Coherence in Photosynthetic Light-Harvesting Systems

ARTICLE *in* JOURNAL OF PHYSICAL CHEMISTRY LETTERS · JULY 2011

Impact Factor: 7.46 · DOI: 10.1021/jz201189p · Source: arXiv

2 AUTHORS, INCLUDING:

Paul Brumer
University of Toronto
323 PUBLICATIONS **8,211** CITATIONS

The Physical Basis for Long-lived Electronic Coherence in Photosynthetic Light Harvesting Systems

Leonardo A. Pachón and Paul Brumer
Chemical Physics Theory Group, Department of Chemistry and Center for Quantum Information and Quantum Control, University of Toronto, Toronto, Canada M5S 3H6

The physical basis for observed long-lived electronic coherence in photosynthetic light-harvesting systems is identified using an analytically soluble model. Three physical features are found to be responsible for their long coherence lifetimes: i) an *effective* low temperature regime and its implicit non-Markovian character, ii) the small energy gap between excitonic states, and iii) the small ratio of the energy gap to the coupling between excitonic states. Using this approach, we obtain decoherence times for a dimer model with FMO parameters of ≈ 160 fs at 77 K and ≈ 80 fs at 277 K. As such, significant oscillations are found to persist for 600 fs and 300 fs, respectively, in accord with the experiment and with previous computations. Similar good agreement is found for PC645 at room temperature, with oscillations persisting for 400 fs. The analytic expressions obtained provide direct insight into the parameter dependence of the decoherence time scales.

Introduction.—Electronic energy transfer is ubiquitous in nature and its dynamics and manipulation is of special interest in diverse fields of physics, chemistry, biology and engineering. Under natural conditions loss of coherence is expected to occur on ultrashort times scale due to interaction with the environment. For example, results on betaine dye molecules [1] and on femtosecond dynamics and laser control of charge transport in trans-polyacetylene [2] suggest that these time scales are very short, $\sim$2.5 fs and $\sim$3.7 fs, respectively. At high temperatures and for weak coupling to the environment, a classical treatment of the thermal fluctuations suggests that this time scale can be determined as $\tau_{\rm G} = \sqrt{\hbar^2/2\lambda k_{\rm B}T}$ where λ is the system reorganization energy [3, 4]. Based on this expression, the dephasing time for photosynthetic complexes, the systems of interest in this paper, (wherein a typical value of the reorganization energy is $\lambda = 130$ cm^{-1}), can be estimated [5] to be $\tau_{\rm G} = 45$ fs at $T = 77$ K and $\tau_{\rm G} = 23$ fs and $T = 294$ K.

By contrast, recent experiments in photosynthetic complexes such as the FMO complex [6, 7] and the PC645 complex [8] have found that electronic coherences among different chromophores survive up to 800 fs at 77 K [6] and up 400 fs at room temperature [7, 8]. This surprising observation and its possible consequences for biological processes have been discussed extensively [5–14] and very elaborate models have been developed in order to understand the underlying dynamics [10–14]. Interestingly, despite the diversity of approaches and techniques, most [5, 8–14] now predict long-lived coherences on the same times scales as found experimentally [6–8]. This suggests that the underlying physical features are correctly contained in these approaches. However, the sheer complexity of these computations has prevented one from identifying these essential physical features.

In this paper we present a simple analytic approach that provides deep insights into the long lived coherences in the evolution of FMO complexes [5–11, 13] and PC645 [8, 12] and allows for the identification of central characteristics responsible for these long lived coherences. Our analysis identifies the small *effective* temperature of the system (see below), the very small, but nonzero, energy gap between exciton states, and their coupling as the basic elements behind these long lifetimes. Given these conditions, we show that the lifetimes are not "surprisingly long". As such, the challenge now reverts to obtaining an atomistic understanding [13] of the origins of these parameter values.

Model.—Consider first results for the Fenna-Matthews-Olson (FMO) complexes, in particular the FMO pigment-protein complex from *Chlorobium tepidum* [6, 7]. This is a trimer consisting of identical, weakly interacting monomers [15]. Each weakly interacting FMO monomer contains seven coupled bacteriochlorophyll-*a* (BChl*a*) chromophores arranged asymmetrically, yielding seven nondegenerate, delocalized molecular excited states (excitons) [6, 7]. Since the electronic coupling between the BChl*a* 1 and BChl*a* 2 is relatively strong in comparison with the other coupling strengths [15], we can approximate the dynamics of the excitation as given by a dimer composed by BChl*a* 1 and BChl*a* 2. This, often adopted, approximation is utilized below.

We consider the dimer (see Fig. 1) to be described by the Hamiltonian [16, 17]

$$\begin{aligned} H = &\frac{\hbar}{2}\epsilon_1\sigma_{z,1} + \frac{\hbar}{2}\epsilon_2\sigma_{z,2} + \frac{\hbar}{2}\Delta\left(\sigma_{x,1}\sigma_{x,2} + \sigma_{y,1}\sigma_{y,2}\right) \\ &+ \frac{\hbar}{2}\delta\mu_1\sigma_{z,1}R_1 + \frac{\hbar}{2}\delta\mu_2\sigma_{z,2}R_2 + B_1 + B_2, \end{aligned} \tag{1}$$

where $R_i = \sum_\alpha C_{\alpha,i}\left(a_{\alpha,i} + a^\dagger_{\alpha,i}\right)$ is the reaction field operator for molecule i, $B_i = \sum_\alpha \hbar\omega_{\alpha,i}a^\dagger_{\alpha,i}a_{\alpha,i}$ is the energy stored in the solvent cage of molecule i and $\delta\mu_j$ is the difference between the dipole moment of the chromophore j in the ground and excited states [16, 17]. The first two terms in Eq. (1) are the individual sites and the third term is the Δ coupling between them. The subsequent

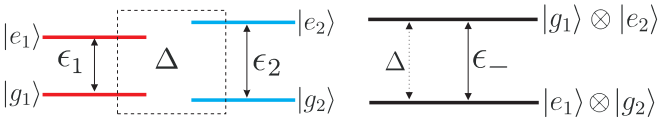

FIG. 1. Left hand side: The pair of interacting chromophores. Right hand side: the effective light harvesting two-level system formed from the pair of interacting chromophores [17, 18].

terms describe the system-bath coupling. Following [17, 18], the Hamiltonian (1) can be written with respect to the basis $\{|g_1\rangle \otimes |g_2\rangle, |g_1\rangle \otimes |e_2\rangle, |e_1\rangle \otimes |g_2\rangle, |e_1\rangle \otimes |e_2\rangle\}$ describing the state of the two chromophores, i.e.

$$H = \sum_{\substack{\alpha \\ i=1,2}} \hbar\omega_{\alpha,i} a^\dagger_{\alpha,i} a_{\alpha,i} \qquad (2)$$
$$+ \frac{\hbar}{2} \begin{pmatrix} -(\epsilon_+ + V_+) & 0 & 0 & 0 \\ 0 & -(\epsilon_- + V_-) & 2\Delta & 0 \\ 0 & 2\Delta & \epsilon_- + V_- & 0 \\ 0 & 0 & 0 & \epsilon_+ + V_+ \end{pmatrix},$$

where $\epsilon_\pm \equiv \epsilon_1 \pm \epsilon_2$, and $V_\pm \equiv \delta\mu_1 R_1 \pm \delta\mu_2 R_2$.

Since under excitation by weak light only the singly excited states need to be taken into account, we can identify [17, 18] the active environment coupled 2D-subspace as $\{|e_1\rangle \otimes |g_2\rangle, |g_1\rangle \otimes |e_2\rangle\}$. In this central subspace of (2), the effective interacting biomolecular two-level system Hamiltonian reads

$$H = \left(\frac{\hbar\epsilon}{2}\sigma_z + \hbar\Delta\sigma_x\right) + \frac{\hbar}{2}\sigma_z V + \sum_{\substack{\alpha \\ i=1,2}} \hbar\omega_{\alpha,i} a^\dagger_{\alpha,i} a_{\alpha,i} \qquad (3)$$

where $\epsilon \equiv \epsilon_-$ and $V \equiv V_-$. This is schematically illustrated in Fig. 1, where Δ is the associated "tunneling energy", between the new basis states $|e_1\rangle \otimes |g_2\rangle$ and $|g_1\rangle \otimes |e_2\rangle$.

Given the biophysical nanostructure composition [17], we can assume that the two bath are uncorrelated $[a_{\alpha,1}, a^\dagger_{\alpha,2}] = 0$, which implies that $\langle R_1(t'')R_2(t')\rangle = \langle R_2(t'')R_1(t')\rangle = 0$. Hence, (3) can be written in the standard form of the spin-boson model [17]

$$H = \left(\frac{\hbar\epsilon}{2}\sigma_z + \hbar\Delta\sigma_x\right) + \frac{\hbar}{2}\sigma_z \sum_\beta g_\beta(b_\beta + b^\dagger_\beta) + \sum_\beta \hbar\omega_\beta b^\dagger_\beta b_\beta \,, \qquad (4)$$

where the b_β includes harmonic oscillators coupled to both chromophores, with couplings g_β.

The environment is fully characterized by the spectral density $J(\omega) = \sum_\alpha g^2_\alpha \delta(\omega - \omega_\alpha)$, being a quasi-continuous function for typical condensed phase applications that determines all bath-correlations that are relevant for the system [19, 20]. For Ohmic dissipation $J(\omega) = 2K\omega\, \mathrm{e}^{-\omega/\omega_\mathrm{C}}$, where the dimensionless parameter K describes the damping strength and ω_C is the cut-off frequency [19, 20]. An Ohmic spectral density is a useful choice for, e.g. electron transfer dynamics or biomolecular complexes [17, 21]. The parameter K is related to the reorganization energy λ by means of $\lambda = 2K\hbar\omega_\mathrm{C}$ and the phonon relaxation time is given by $\tau = \pi/(2\omega_\mathrm{C})$ [10, 19].

Hamiltonian (4) has been extensively studied in literature (cf. Chaps. 18-22 in [19] and references therein). The parameter range within which the light harvesting systems of interest lie allows for the use of the non-interacting blip approximation (NIBA). This approximation is valid for weak system-bath coupling and for $\epsilon/2\Delta < 1$, over the whole range of temperatures (see Chap. 21 in [19]), and provides simple and accurate analytic expressions for relaxation and decoherence rates.

In the case of FMO, the energy gap ϵ is $(315 - 240)$ cm^{-1} while the coupling energy Δ corresponds to 87.7 cm^{-1} (see [10, 14] and references therein). According to [10, 14], the reorganization energy in this case is $\lambda \approx 35$ cm^{-1} and the phonon relaxation time is $\tau = 50$ fs. Hence, for this case we get $K = \lambda/(2\hbar\omega_\mathrm{C}) = \lambda\tau/(\hbar\pi) = 0.105$. Additionally, at $T = 77$ K, $2\Delta/k_\mathrm{B}T \approx 3.28$ while at $T = 277$ K, $2\Delta/k_\mathrm{B}T \approx 0.911$. Table I summarizes the parameters of the present analysis, where we have used the same ω_C value at both temperatures. Clearly these parameters place the system within the domain of accuracy of the NIBA approach.

$\epsilon/2\Delta$	K	$2\Delta/\omega_\mathrm{C}$	$2\Delta/k_\mathrm{B}T$
0.428	0.105	1.052	3.28
0.428	0.105	1.052	0.911

TABLE I. Parameters used for dimer formed of BChl$a$ 1 and BChl$a$ 2 at $T = 77$ K (first row) and $T = 277$ K (second row).

The high temperature limit in this approach is given by temperatures well in excess of $T_\mathrm{b} = \hbar(\Delta^2_\mathrm{eff} + \epsilon^2)^{1/2}/k_\mathrm{B}$, where

$$\Delta_\mathrm{eff} = [\Gamma(1-2K)\cos(\pi K)]^{1/2(1-K)} (\Delta/\omega_\mathrm{c})^{K/(1-K)} \Delta.$$

For the set of parameters listed in Table I, we find $T_\mathrm{b} \approx 288$ K. Hence the FMO experiments, at 77 K and 277 K, are in the low temperature regime, $T < T_\mathrm{b}$. In this regime, the Rabi frequency Ω, the relaxation rate γ_r and the decoherence rate γ are given by [19]

$$\Omega^2 = \Delta^2_\mathrm{eff}[1 - 2\Re u(\mathrm{i}\Delta_\mathrm{b})] + \epsilon^2 \qquad (5)$$

$$\gamma_\mathrm{r} = \frac{\pi}{2}\frac{\Delta^2_\mathrm{eff}}{\Delta^2_\mathrm{b}} S(\Delta_\mathrm{b}) \qquad (6)$$

$$\gamma = \frac{\gamma_\mathrm{r}}{2} + \frac{\pi}{2} K \frac{\epsilon^2}{\Delta^2_\mathrm{b}} S(0), \qquad (7)$$

respectively, where $\Delta_\mathrm{b} = \sqrt{\Delta^2_\mathrm{eff} + \epsilon^2}$, $u(z) = \frac{1}{2}\int_0^\infty \mathrm{d}\omega \frac{J(\omega)}{\omega^2 + z^2}(\coth(\hbar\omega/2k_\mathrm{B}T) - 1)$ and $S(\omega) =$

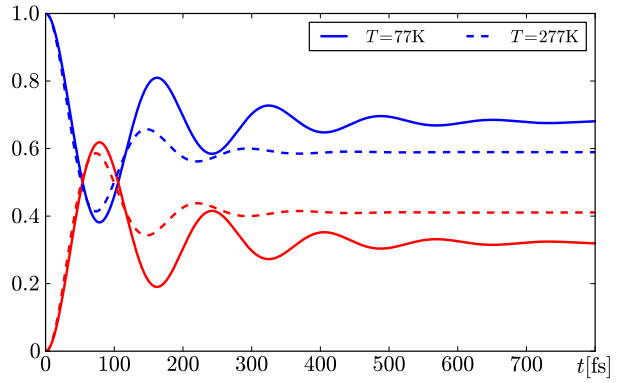

FIG. 2. Time evolution of the population of the electronic manifolds $|e_1\rangle\otimes|g_2\rangle\langle g_2|\otimes\langle e_1|$ (blue curve) and $|g_1\rangle\otimes|e_2\rangle\langle e_2|\otimes\langle g_1|$ (red curve) for the FMO dimer formed of BChl*a* 1 and BChl*a* 2 using the parameters displayed in Table I. Continuous lines depict the evolution at $T = 77$ K whereas dashed lines are at $T = 277$ K. We assume that at $t = 0$, the full excitation is localized in $|e_1\rangle \otimes |g_2\rangle\langle g_2| \otimes \langle e_1|$.

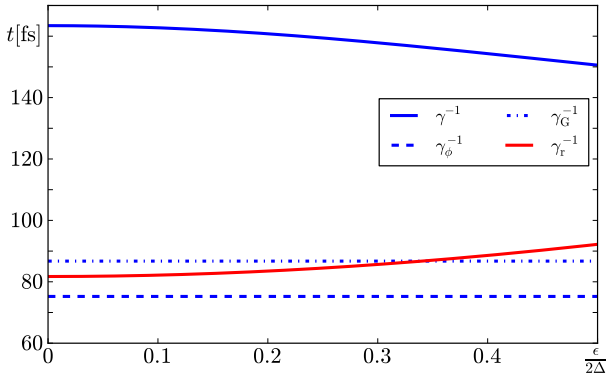

FIG. 3. Relaxation time γ_r^{-1} (red line) and decoherence time γ^{-1} (continuous blue line) as functions of $\epsilon/2\Delta$, for fixed $\Delta = 35$ cm^{-1}. The dashed blue line, $\gamma_\phi = 2\pi(k_BT/\hbar)\lambda/\hbar\omega_C$, denotes the dephasing rate used in [4, 7, 9] and the dotdashed blue line denotes the decoherence time $\tau_G = \sqrt{\hbar^2/2\lambda k_BT}$ used in [3–5]. Fixed parameters as in Table I.

$J(\omega)\coth(\hbar\omega/2k_BT)$ is the noise power. Non-Markovian corrections are already included in Eqs. (5)-(7). For the particular case of Ohmic dissipation adopted here [19],

$$\Omega^2 = \Delta_b^2 + 2K\Delta_{eff}^2\left[\Re\psi(i\hbar\Delta_b/2\pi k_BT) - \ln(\hbar\Delta_b/2\pi k_BT)\right] \quad (8)$$

$$\gamma_r = \pi K\coth(\hbar\Delta_b/2k_BT)\Delta_{eff}^2/\Delta_b, \quad (9)$$

$$\gamma = \gamma_r/2 + 2\pi K(\epsilon^2/\Delta_b^2)k_BT/\hbar, \quad (10)$$

where $\psi(z)$ is the digamma function. Equations (9) - (10) provide simple analytic expressions for the desired rates.

With this set of expressions, and the parameters given in Table I, we find $2\pi\Omega^{-1} = 163$ fs, $\gamma_r^{-1} = 90$ fs, $\gamma^{-1} = 153$ fs at $T = 77$ K, while $2\pi\Omega^{-1} = 151$ fs, $\gamma_r^{-1} = 45$ fs, $\gamma^{-1} = 69$ fs at $T = 277$ K. Despite the simplicity of the model, the resultant dynamics [given analytically in Eqs. (21.170) and (21.173) of Ref. [19]] is depicted in Fig. 2 and describes the survival of coherences on the correct time scale and in good qualitative agreement with recent results. Quantitative agreement could be achieved by small changes in τ and/or ω_C. In Fig. 2, only the decay of the excitations is absent, since coupling to other chromophores [10, 13, 14] is here neglected.

To examine the parameter dependence, Fig. 3 shows the relaxation rate γ_r and the decoherence rate γ as a function of the energy splitting, ϵ, for fixed Δ, using the parameters displayed in Table I. Clearly in this "low temperature regime" (8)-(10), i.e., $T < T_b$, the larger the ratio $\epsilon/2\Delta$ the shorter the dephasing time and concomitantly the longer the relaxation time. These time scales are also compared in Fig. 3 with the ones predicted by $\gamma_\phi = 2\pi(k_BT/\hbar)\lambda/\hbar\omega_C$ used in [4, 7, 9] and with $\gamma_G = 1/\tau_G$ discussed earlier, both of which are clearly far too short.

As a second example we consider results on marine algae [5], in particular the results for PC645, which has been studied experimentally [8], and numerically in great detail [12]. PC645 contains eight bilin molecules covalently bound to the protein scaffold. A dihydrobiliverdin (DBV) dimer is located at the center of the complex and two mesobiliverdin (MBV) molecules located near the protein periphery give rise to the upper half of the complex absorption spectrum. Excitation of this dimer initiates the light harvesting process [8]. The electronic coupling between the closely spaced DBVc and DBVd molecules is ∼320 cm^{-1} and this relatively strong coupling results in delocalization of the excitation, yielding the dimer electronic excited states labelled DBV+ and DBV−. Excitation energy absorbed by the dimer flows to the MBV molecules which are each 23 Å from the closest DBV, and ultimately to four phycocyanobilins (PCB) that absorb in the lower-energy half of the absorption spectrum [8].

The exciton states related to DBVc and DBVd are mainly composed of DBV− and DBV+ that are antisymmetric and symmetric linear combinations of the DBV sites, though they also contain small contributions from the other bilin sites [12]. This allows us to concentrate only on a dimer, as in the previous example, but here formed of DBVc and DBVd. In this case, a Debye-Ohmic spectral density, $J(\omega) = 2\lambda\omega\tau/(1+\omega^2\tau^2)$, is more appropriate [12].

For the chromophores DVBc and DVBd the energy gap is $(17116 - 17034)$ cm^{-1} with the coupling energy corresponding to 319.4 cm^{-1} [8, 12]. In accord with [12], the reorganization energy λ in this case is ∼130 cm^{-1}, with

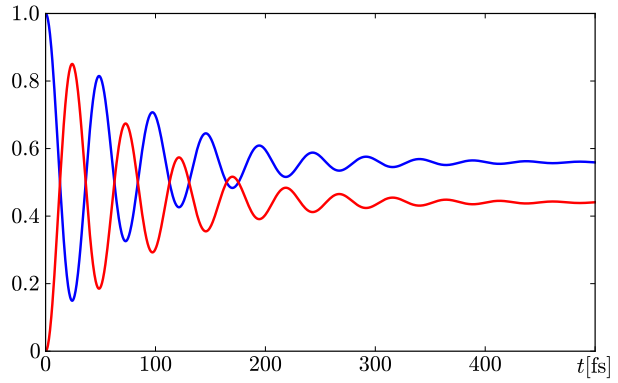

FIG. 4. Time evolution of the population of the electronic manifolds $|e_1\rangle\otimes|g_2\rangle\langle g_2|\otimes\langle e_1|$ (blue curve) and $|g_1\rangle\otimes|e_2\rangle\langle e_2|\otimes\langle g_1|$ (red curve) for the PC645 DVB-dimer.

the shorter of two relaxation times being $\tau = 50$ fs. Additionally, at $T = 294$ K, the temperature at which the experiment was performed, $2\Delta/k_{\rm B}T = 3.1262$. For this set of parameters, we have $T_{\rm b} \sim 926$ K, a high temperature that is consistent with the high frequencies involved in the present case [22]. Hence the PC645 experiment, at room temperature, is also in the effective low temperature $T < T_{\rm b}$ domain. For the case of the Debye-Ohmic spectral density we have (via a relatively simple numerical computation) that $2\pi\Omega^{-1} = 49$ fs, $\gamma_{\rm r}^{-1} = 76$ fs, $\gamma^{-1} = 88$ fs with the associated evolution shown in Fig. 4. These results are in very good qualitative agreement with both the long lived experimental coherence time scales and with the recent intricate solution to the master equations [12].

Considering that the long time scales emerge naturally here from the system parameters, why were far shorter decoherence time scales originally expected for these systems? To see this, note that in molecular systems, dynamics is often studied between different electronic eigenstates of the system, separated by greater than $\sim 10^4$ cm^{-1}, with no coupling between them. In such cases, the dephasing time from Eqs. (9) - (10) would be extremely short. By contrast, in the case of photosynthetic complexes, energy transfer occurs between exciton states that are close in energy and additionally are coupled. This generates a small value for the ratio ϵ/Δ which in turn is responsible for longer dephasing times (see Fig. 3). Additionally, expression such as $\tau_{\rm G}$, which are often used to estimate rates, are only valid at high temperature, $k_{\rm B}T \gg \hbar\omega_{\rm C}$, and at short times, $t < \omega_{\rm C}^{-1}$. Under conditions when the expression for $\tau_{\rm G}$ is valid, the bath modes can be treated classically [23], as in [1, 2]. When one is not in the appropriate regime, the classical evolution of the bath underestimates quantum coherent effects [23] because at low temperatures quantum fluctuations overcome thermal fluctuations [3]. Hence, estimates based on τ_G are unreliable. Similarly, $\gamma_\phi = 2\pi(k_{\rm B}T/\hbar)\lambda/\hbar\omega_{\rm C}$ estimates also provide an inadequate representation of the true physics and associated dependence on system and bath parameters, and result in decoherence times that are severely underestimated and misleading.

Summary. A proper spin-boson treatment of electronic energy transfer in model photosynthetic light harvesting systems has been shown to give *analytic* results with long coherence lifetimes that are in very good agreement with experiment and with other, far far more complex, computations. The analytic form allows an analysis of the parameter dependence of the decoherence times, and shows that the observed long lifetimes arise naturally in the effective low temperature regime and for appropriate ratios of the energy splitting to the coupling strength.

This work was supported by the US Air Force Office of Scientific Research under contract number FA9550-10-1-0260.

[1] H. Hwang and P. J. Rossky, J. Phys. Chem. B **108**, 6723 (2004).
[2] I. Franco, M. Shapiro, and P. Brumer, J. Chem. Phys. **128**, 244905 (2008).
[3] H. Hwang and P. J. Rossky, J. Chem. Phys. **120**, 11380 (2004).
[4] J. B. Gilmore and R. H. McKenzie, J. Phys. Chem. A **112**, 2162 (2008).
[5] Y.-C. Cheng and G. R. Fleming, Ann. Rev. Phys. Chem. **60**, 241 (2009).
[6] G. S. Engel, T. R. Calhoun, E. L. Read, T.-K. Ahn, T. Mančal, Y.-C. Cheng, R. E. Blankenship, and G. R. Fleming, Nature **446**, 782 (2007).
[7] G. Panitchayangkoon, D. Hayes, K. A. Fransted, J. R. Caram, E. Harel, J. Wen, R. E. Blankenship, and G. S. Engel, Proc. Natl. Acad. Sci. USA **107**, 12766 (2010).
[8] E. Collini, C. Y. Wong, K. E. Wilk, P. M. G. Curmi, P. Brumer, and G. D. Scholes, Nature **463**, 644 (2010).
[9] P. Rebentrost, M. Mohseni, I. Kassal, S. Lloyd, and A. Aspuru-Guzik, New J. Phys. **11**, 033003 (2009).
[10] A. Ishizaki and G. R. Fleming, Proc. Natl. Acad. Sci. USA **106**, 17255 (2009).
[11] J. S. Briggs and A. Eisfeld, Phys. Rev. E **83**, 051911 (2011).
[12] P. Huo and D. F. Coker, J. Phys. Chem. Lett. **2**, 825 (2011).
[13] S. Shim, P. Rebentrost, S. Valleau, and A. Aspuru-Guzik, (2011), arXiv:1104.2943v1.
[14] P. Nalbach, D. Braun, and M. Thorwart, (2011), arXiv:1104.2031v1.
[15] J. Adolphs and T. Renger, Biophys. J. **91**, 2778 (2006).
[16] J. B. Gilmore and R. H. McKenzie, J. Phys.: Condens. Matter **17**, 1735 (2005).
[17] J. B. Gilmore and R. H. McKenzie, Chem. Phys. Lett. **421**, 266 (2006).
[18] J. Eckel, J. H. Reina, and M. Thorwart, New J. Phys. **11**, 085001 (2009).
[19] U. Weiss, *Quantum Dissipative Systems*, 3rd ed. (World

Scientific, Singapore, 2008).
[20] A. J. Leggett, S. Chakravarty, A. T. Dorsey, M. P. A. Fisher, A. Garg, and W. Zwerger, Rev. Mod. Phys. **59**, 1 (1987).
[21] V. May and O. Kühn, *Charge and energy transfer dynamics in molecular systems* (Berlin: Wiley, 2001).
[22] F. Galve, L. A. Pachón, and D. Zueco, Phys. Rev. Lett. **105**, 180501 (2010).
[23] M. Thoss, H. Wang, and W. H. Miller, J. Chem. Phys. **115**, 2991 (2001).